

Published in final edited form as:

*Nat Med.* 2012 May ; 18(5): 766–773. doi:10.1038/nm.2693.

## RBM20, a gene for hereditary cardiomyopathy, regulates titin splicing

Wei Guo<sup>1,10</sup>, Sebastian Schafer<sup>2,10</sup>, Marion L. Greaser<sup>1</sup>, Michael H. Radke<sup>3</sup>, Martin Liss<sup>3</sup>, Thirupugal Govindarajan<sup>3</sup>, Henrike Maatz<sup>2</sup>, Herbert Schulz<sup>2</sup>, Shijun Li<sup>1</sup>, Amanda M. Parrish<sup>1</sup>, Vita Dauksaite<sup>3</sup>, Padmanabhan Vakeel<sup>3</sup>, Sabine Klaassen<sup>4</sup>, Brenda Gerull<sup>4</sup>, Ludwig Thierfelder<sup>4</sup>, Vera Regitz-Zagrosek<sup>5</sup>, Timothy A. Hacker<sup>6</sup>, Kurt W. Saupe<sup>6</sup>, G. William Dec<sup>7</sup>, Patrick T. Ellinor<sup>7</sup>, Calum A. MacRae<sup>7</sup>, Bastian Spallek<sup>8</sup>, Robert Fischer<sup>8</sup>, Andreas Perrot<sup>9</sup>, Cemil Özcelik<sup>9</sup>, Kathrin Saar<sup>2</sup>, Norbert Hubner<sup>2</sup>, and Michael Gotthardt<sup>3</sup>

<sup>1</sup>Muscle Biology Laboratory, University of Wisconsin-Madison, Madison, Wisconsin 53706, USA

<sup>2</sup>Max-Delbrück-Center for Molecular Medicine, 13125 Berlin, Germany

<sup>3</sup>Neuromuscular and Cardiovascular Cell Biology, Max-Delbrück-Center for Molecular Medicine, 13125 Berlin, Germany

<sup>4</sup>Cardiovascular Molecular Genetics, Max-Delbrück-Center for Molecular Medicine, 13125 Berlin, Germany

<sup>5</sup>Institute of Gender in Medicine and Center for Cardiovascular Research, Charité-University Medicine Berlin, 13353 Berlin, Germany

<sup>6</sup>Department of Medicine, University of Wisconsin-Madison, Madison, Wisconsin 53706, USA

<sup>7</sup>Cardiology Division, Massachusetts General Hospital, Charlestown, Massachusetts 02129, USA

<sup>8</sup>Universitätsklinikum Benjamin Franklin, Charité-University Medicine Berlin, 12203 Berlin, Germany

<sup>9</sup>Department of Cardiology (Campus Virchow-Klinikum), Charité-University Medicine Berlin, 13353 Berlin, Germany.

### Abstract

Alternative splicing plays a major role in the adaptation of cardiac function exemplified by the isoform switch of titin, which adjusts ventricular filling. We previously identified a rat strain deficient in titin splicing. Using genetic mapping, we found a loss-of-function mutation in RBM20 as the underlying cause for the pathological titin isoform expression. Mutations in human RBM20 have previously been shown to cause dilated cardiomyopathy. We showed that the phenotype of Rbm20 deficient rats resembles the human pathology. Deep sequencing of the human and rat

**Corresponding author** Correspondence and requests for materials should be addressed to M.G. (gotthardt@mdc-berlin.de).

<sup>10</sup>These authors contributed equally to this work

**Author Contributions** M.L.G., N.H., and M.G. designed the research. W.G., S.S., M.H.R., M.L., T.G., H.M., H.S., S.L., A.M.P., V.D., P.V., S.K., B.G., L.T., V.R.-Z., T.A.H., K.W.S., G.W.D., P.T.E., C.A.M., B.S., R.F., A.P., C.O., K.S., performed the research. W.G., S.S., M.L.G., H.S., W.G., S.S., M.H.R., M.L., T.G., H.M., H.S., S.L., A.M.P., V.D., P.V., S.K., B.G., L.T., V.R.-Z., T.A.H., K.W.S., G.W.D., P.T.E., C.A.M., B.S., R.F., A.P., C.O., K.S., and M.G. performed data analysis. W.G., T.G., H.M., H.S., S.L., A.M.P., V.D., P.V., S.K., B.G., L.T., V.R.-Z., T.A.H., K.W.S., G.W.D., P.T.E., C.A.M., B.S., R.F., A.P., C.O., and K.S. provided discussion and advice. V.R.-Z., A.P., C.O. provided patient material; S.S., M.H.R., T.G., H.S., M.G. performed bioinformatics analysis. S.S., M.L.G., M.H.R., N.H., and M.G. wrote the paper.

**Note:** Supplementary Information is available on the Nature Medicine Website.

### Competing financial interests

The authors declare no competing financial interests.

cardiac transcriptome revealed an RBM20 dependent regulation of alternative splicing. Additionally to titin we identified a set of 30 genes with conserved regulation between human and rat. This network is enriched for genes previously linked to cardiomyopathy, ion-homeostasis, and sarcomere biology. Our studies emphasize the importance of posttranscriptional regulation in cardiac function and provide mechanistic insights into the pathogenesis of human heart failure.

---

RNA-splicing is the removal of intervening sequences (introns) from mRNA precursors. It involves the spliceosome and the dynamic interaction of RNA and protein complexes<sup>1</sup>. The process is tightly regulated by proteins that repress or activate splice site selection – among them SR-proteins and SR related factors (Arg/Ser domain containing proteins), which modulate binding and assembly of the spliceosome complex and thus determine differential inclusion of exons in the mature transcript<sup>2</sup>. Few mutations in spliceosome components have been described, suggesting that the resulting defects are incompatible with life<sup>3</sup>, and only a small number of human diseases have been attributed to the *trans* effects of mutations in RNA binding proteins – largely cancer, neurological diseases, and muscular atrophy<sup>4</sup>. Nevertheless, a substantial number of variants have been identified in splice consensus sites (*cis*-effects) representing the underlying cause of a range of disorders including cardiac disease<sup>5</sup>.

Multiple changes in gene and isoform expression relate to both adaptations in cardiac physiology and to cardiac disease, among them alternative splicing of the giant protein titin. Titin is a sarcomeric protein that determines the structure and biomechanical properties of striated muscle, and it has been associated with human cardiac disease<sup>6</sup>. Both alternative splicing<sup>7-10</sup> and post-translational modification tune titin-based passive tension, an important contributor to efficient ventricular filling<sup>11,12</sup>. Titin phosphorylation in response to adrenergic stimulation has been attributed to protein kinase A (PKA) acting on the elastic N2B region<sup>11</sup>, but despite established links between the alternative splicing of titin and both thyroid hormone and insulin signaling<sup>13-15</sup>, the splice factors that determine titin isoform transitions are still unknown.

Here we used a spontaneously occurring rat strain deficient in titin splicing with persistent expression of a giant titin isoform (N2BA-G)<sup>16</sup> in adult cardiac tissue. We used genome-wide mapping approaches to identify RNA binding motif protein 20 (Rbm20) as the underlying factor that was associated with the regulation of titin splicing. Interestingly, human RBM20 has recently been linked to human dilated cardiomyopathy (DCM)<sup>17,18</sup>, but the function, regulation, and substrates of RBM20 remain unknown. We show that RBM20 deficiency in rats leads to many clinical features that are observed in patients with cardiomyopathy related to RBM20 mutations; namely, ventricular enlargement, arrhythmia, increased rate of sudden death, and extensive fibrosis. This suggests a conserved RBM20 mediated cardiac pathology in both species. We demonstrate that RBM20 regulates cardiac isoform expression and binds RNA. Moreover, we analyzed the global effect of RBM20 deficiency on alternative splicing in rat and human DCM with and without an RBM20 missense mutation. Our studies document significant overlap of posttranscriptionally regulated genes that depend on RBM20. This includes titin and a network of 30 additional genes, which show RBM20 genotype dependent alternative splicing in rat and human. Our studies not only offer mechanistic insights but also provide functional annotation of RBM20 substrates that contribute to cardiomyopathy and heart failure, a major source of mortality in the developed world.

## RESULTS

### Identification of the SR-related protein Rbm20 as an effector of titin isoform expression

We utilized a backcross between rats deficient in titin splicing (*titin<sub>mut</sub>*)<sup>16,19</sup> and the Brown Norway (BN) reference and identified a ~2 Mbp interval on Chromosome 1q55 that contains 9 genes (Fig.1a; Supplement Fig.1). Sequence analysis of the coding regions showed that only Rbm20 differed between unaffected and affected rats with a 95 kb deletion that removes exons 2–14 in the latter. The missing exons encode the RNA binding motif-, the RS-, and the Zn<sup>2+</sup> finger domains. We confirmed the deletion by Southern blot, qRT-PCR, and Western blot in hetero- and homozygous Rbm20 deficient rats (Fig.1b–d). In addition, we genotyped the Rbm20 deletion in all 191 animals from two independent backcrosses demonstrating complete co-segregation between the titin splice defect and the Rbm20 mutation (Supplement Fig.1a). Finally, we used adenoviral gene delivery to re-express Rbm20 in deficient cardiomyocytes and reconstituted expression of the short titin isoform (Fig.1e–g). The combination of rodent genetics and the reversion of the splice deficient phenotype established Rbm20 as a trans-acting factor regulating titin isoform expression.

### RBM20 regulates alternative splicing and is expressed in striated muscle

Towards understanding the physiological functions of RBM20, we investigated its role in alternative splicing on the molecular level. Within the nucleus Rbm20 partially colocalizes with the splice factors Ptp1 and U2AF65 (Fig.2a). The latter also contains an RS domain that mediates its recruitment to sites of active splicing<sup>20</sup>. We demonstrated that Rbm20 binds total RNA by crosslinking and immunoprecipitation experiments (Fig.2b). Moreover, we confirmed the specific activity of Rbm20 on titin RNA in a splice reporter assay where exclusion of titin PEVK exons results in reduced reporter activity (Fig.2c). The assay was validated on the RNA level and provides a robust readout of Rbm20 activity (Supplement Fig.2). In both myoblasts (C2C12) and fibroblasts (HEK 293) expression of Rbm20 led to exclusion of the PEVK exon 8 containing the firefly luciferase reporter (Fluc – Fig.2d). Thus, Rbm20 is sufficient to drive alternative splicing of titin's PEVK region in muscle or non-muscle cells and does not rely on a cardiac specific cofactor. Co-transfection of the splice reporter and expression constructs encoding the splice factors PTBP1 or HuD<sup>21,22</sup> was used to exclude non-specific effects of RNA binding proteins (Fig.2e). Rbm20 stoichiometrically affects splicing of titin's PEVK region with increased levels leading to increased exclusion of exons (Fig.2f). Rbm20 is predominantly expressed in striated muscle with the highest levels in the heart (Fig.2g). In differentiating myoblasts, Rbm20 expression correlates with sarcomere assembly (Fig.2h). It peaks when  $\alpha$ -actinin is largely localized in mature Z-bodies within the nascent myofiber (punctuate  $\alpha$ -actinin staining) and declines as sarcomeres continue to mature (Fig.2i). Experimental cardiomyopathies in mice – both genetic and viral – did not affect RBM20 expression (Supplement Fig.3).

### Rats and humans share RBM20-dependent pathology with cardiomyopathy, fibrosis, and arrhythmia

Heterozygous and homozygous Rbm20 null alleles resulted in left ventricular dilatation as determined by echocardiography in adult animals. While left ventricular diastolic diameter (LVDD) was significantly increased, there were no changes in systolic ventricular dimensions or contractility indices including fractional shortening (Fig.3a,b).

The sub-endocardial fibrosis increases with age and is accompanied by electrical abnormalities such as widening of the QRS complex, atrioventricular conduction delay, and a predisposition to arrhythmia (Fig.3c–f, Supplement Fig.4–6). Both Rbm20 deficient rats and humans with RBM20 mutations<sup>17,18</sup> can experience sudden death that occurs well after

adolescence. Thus, Rbm20 deficient rats mirror the pathological features of the previously reported corresponding human disease<sup>17,18</sup> (Supplement Table S1).

### Aberrant splicing of titin in a DCM patient with a novel RBM20 missense mutation

To validate RBM20 dependent titin splicing and its relevance for human disease, we investigated an individual with a heterozygote S635A mutation in RBM20. The mutation resides in the RS domain in an evolutionary highly conserved region (Fig.4a, b). The 34-year old subject suffered from severe cardiomyopathy with a clinical presentation that corroborates recently published patient data<sup>17,18</sup>. We tested 3,000 alleles from ethnically matched individuals without cardiomyopathy as controls and were unable to detect this variant (it has not been reported in dbSNP or the 1,000's genomes project, indicating that the variant is not a frequent polymorphism). Finally, we demonstrated that our newly identified S635A mutation along with all known human RBM20 mutations<sup>17,18</sup> has functional effects using our reporter assay. We found complete loss of function for all mutations analyzed except for the conserved amino-acid change V535I caused by the only mutation outside exon 9 (Fig.4d).

After informed consent we obtained cardiac biopsy material from the individual with the S635A mutation and cardiac tissue from two subjects with cardiomyopathy after cardiac transplantation that did not carry any non-synonymous sequence variants in RBM20 (as determined by Sanger sequencing of the entire coding region). On the protein level we found that the heterozygote RBM20 mutation S635A shifts human titin isoform expression with an increased molecular weight similar to the larger isoform expressed in heterozygous rats. The two subjects with cardiomyopathy that do not carry mutations in RBM20 expressed N2B and N2BA titins of lower molecular weight similar to published patterns found in normal individuals (Fig.4e).

### RBM20 regulates select genes related to cardiac disease, sarcomeric function, and ion transport

We used deep sequencing (Illumina) of the rat and human cardiac transcriptome to refine our analysis of RBM20 dependent splicing. High throughput RNA sequencing generates information on both the gene and exon level, thus facilitating the identification of additional candidate substrates as well as RBM20 dependent isoform composition. We analyzed the cardiac transcriptome of Rbm20 homozygous deficient, heterozygous, and wildtype rats ( $n=3$  per group) versus human DCM with and without mutations in RBM20. The comparison of the different RBM20 genotypes in rat and humans and our analysis of cardiac tissue from relatively young rats (2 month of age) before the onset of cardiomyopathy, minimized potential secondary effects on alternative splicing that are not dependent on RBM20. We generated ~150 million sequencing reads per sample (100bp paired-end; Supplement Fig.7) and found 31 genes with shared RBM20 genotype dependent splicing (False discovery rate [FDR] < 5%) in rats and humans, which is a significantly greater overlap than would be expected by chance ( $P < 10^{-6}$ ). This RBM20 dependent gene network includes titin, whose alternative splicing was expected based on our initial experiments and thus validated our approach. We further confirmed the RNA sequencing results by RT- and qRT-PCR for titin and 6 additional genes (Fig.5, Supplement Fig.8). Gene Ontology analysis of the RBM20 driven network showed enrichment for sarcomere organization and ion transport in the sarcoplasmic reticulum (Fig.5; Supplement Table S2-S5; Supplement Fig.9). The 31 genes show additional enrichment for the Medical Subject Headings "heart failure" and "cardiomyopathy" (MeSH; Fig.5, Supplement Table S6).

Several genes with RBM20 dependent isoform expression show identical splicing patterns on the exon level across species as depicted in Figure 6. Ttn, CaMKII- $\delta$ , Ldb3, and Cacna1c

showed conserved differential splicing of orthologous exons between rat and human for the majority of their alternatively spliced exons (Figs.5+6). Of these, titin was the most extensively miss-spliced gene with long stretches of exons affected – the majority of which were additionally included in RBM20 deficiency. This result is consistent with the expression of larger titin protein isoforms in Rbm20 deficient rats and the individual with the RBM20 S635A mutation (Figs.4+6). The alternatively spliced exons reside in the elastic PEVK- and the immunoglobulin-rich region within the I-band and help explain the increased elasticity of Rbm20-deficient sarcomeres<sup>16</sup>. Furthermore the annotation of constitutive vs. alternative exons facilitated the identification of regions with potential RBM20 binding sites. Here we focus on the 5' splice site at the start of titin's alternatively spliced I-band region (Supplement Fig.10). Using a retention assay we were able to complement our crosslinking and immunoprecipitation derived RNA binding data with the interaction of RBM20 and titin RNA (Supplement Fig.10). For CaMKII $\delta$  exon 14 was spliced out and exons 15 and 16 were included. This caused an isoform shift from CaMKII $\delta$ B to CaMKII $\delta$ A. It should be noted that exon 14 contains the nuclear localization signal. A similar shift has been described in ASF/SF2 deficient animal model with altered excitation contraction coupling that leads to cardiac hypercontractility<sup>22</sup>. LDB3 exon 4 and exon 5/6 are mutually exclusive and are regulated by RBM20. We have found exon 4 to be down regulated in left ventricular tissue from Rbm20 deficient rats and the individual with the RBM20 missense mutation. Cacna1c isoform expression has previously been related to arrhythmia<sup>23</sup> and we find conserved changes in exon inclusion, although at smaller  $\Delta$ PSI levels (PSI: “per cent spliced in”) as compared to the aforementioned genes.

## DISCUSSION

RBM20 has recently been linked to human cardiac disease with mutations in 1.9-3% of individuals with idiopathic DCM<sup>17,18</sup>, but the underlying molecular and pathomechanism have remained elusive. Our multi-faceted analysis of RBM20 function *in vivo* and on the molecular level helps resolve this issue and demonstrates that Rbm20 regulates cardiac isoform expression. Rbm20 deficient rats and humans with RBM20 missense mutations share cardiomyopathy with fibrosis and arrhythmia with sudden death. Our genome-wide transcriptomic analysis revealed a set of 31 RBM20 dependent genes, of which four show remarkable co-regulation down to the exon level (TTN, CAMKII $\delta$ , LDB3, and CACNA1C).

The transcriptomics data was verified on several levels, including the confirmation of concordant protein isoform and RNA isoform expression of rat and human titin. Due to lack of sufficient human biopsy material, we focused our technical validation of the RNA-seq data on the rat. RT-PCR and qRT-PCR analysis confirmed 7 of 14 genes containing exons with a  $\Delta$ PSI >10% (Fig.5). Our deep sequencing analysis with long (100 bp) paired-end-reads that span exon borders, enables the detection of even small changes in isoform regulation with statistical significance that cannot be visualized by RT-PCR ( $\Delta$ PSI < 10%; data not shown). Since RBM20 genotype dependent isoform expression was consistent between species we also consider genes with low  $\Delta$ PSI values as part of the set of RBM20 regulated candidate genes.

Our analysis of titin splice deficient rats revealed a genomic deletion that leads to the loss-of-function of the SR related protein Rbm20. SR and SR related proteins are highly conserved in metazoans<sup>24</sup> and their modular structure with one or two RNA recognition motives (RRM) and an arginine/serine-rich domain (RS) is essential for RNA and protein interactions and thus the recruitment of the splicing machinery<sup>25</sup>. About half of the more than 100 SR related proteins known to date have been implicated in splicing<sup>2</sup>. Regulation of alternative splicing can be achieved by temporal and spatial control of tissue specific expression of RS proteins, or by their posttranslational modification. Similar to its largest

substrate titin, Rbm20 is predominantly expressed in striated muscle (in contrast to most SR related proteins which are ubiquitously expressed) and cardiac expression peaks as myocytes build the sarcomeric structure during differentiation (Fig.2). The difference in the calculated size of ~130 kDa and its migration at ~180 kDa on our PAGE gels implies posttranslational modification. Indeed, SR related proteins are frequently regulated by phosphorylation, resulting in a sizeable difference in molecular weight<sup>26</sup>. Phosphorylation of SR related proteins has previously been associated with reimport into the nucleus<sup>26</sup> and regulation of alternative splicing<sup>27</sup>. Rbm20 is localized in the nucleus throughout myogenic differentiation and was not detected in the cytoplasm (Fig.2h). This would suggest a function in the major (nuclear) spliceosome, where RBM20 regulates isoform expression of genes related to diastolic function, sarcomere assembly, and ion transport as implied by the characterization of its substrate profile with several structural, sarcomeric, enzymatic, and signaling proteins that are alternatively spliced (Fig.5+6).

The availability of rat and human cardiac tissue for analysis of the Rbm20 dependent isoform expression has provided several leads towards understanding the underlying pathomechanism. Our analysis of RBM20 genotype dependent alternative splicing suggests that RBM20 plays a critical role in multiple aspects of cardiac function through a concerted action on genes involved in biomechanics (titin, tropomyosin), ion homeostasis and electrical activity (CAMKII $\delta$ , CACNA1C), and signal transduction (CAMKII $\delta$ , SPEN). Furthermore in addition to titin<sup>6</sup> and CAMKII $\delta$ <sup>28</sup> changes in isoform expression of LDB3 (alias cypher) and CACNA1C have been related to dilated cardiomyopathy or arrhythmia, respectively<sup>29,30</sup>.

Titin is a prominent target of RBM20 and a known cardiomyopathy gene<sup>6,31</sup>. Although altered titin splicing is frequently found in cardiovascular disease<sup>7,32-34</sup>, previously reported changes in titin isoform expression are rather conservative: The altered ratio of N2B and N2BA is not comparable to the excessively large N2BA isoforms produced in RBM20 deficient hearts. This additional increase in titin based elasticity has implications for diastolic function and the Frank Starling mechanism<sup>16</sup>. Furthermore, the reduced recoil associated with a flaccid titin filament could lead to a compensatory increase in collagen biosynthesis and ultimately lead to fibrosis.

Calcium handling is a crucial component of cardiac function and it is affected in all knockouts of cardiac splice factors described so far. Both SC35 and SRp38 deficiency leads to altered Ca<sup>2+</sup> release from the sarcoplasmic reticulum with down-regulation of the ryanodine receptor RyR2<sup>35</sup> and defective splicing of triadin<sup>36</sup>, respectively. Thus, SRp38 and RBM20 share triadin as a substrate. ASF/SF2 and RBM20 both regulate CAMKII $\delta$  isoform expression with the production of a kinase that lacks the nuclear localization signal. It has been shown to be miss-targeted to the sarcolemma, causing not only excitation/contraction coupling defects<sup>37</sup> but also increasing the propensity to ventricular tachycardia. We reported a similar phenotype in Rbm20 deficient rats (Supplement Fig.5).

Moreover mutations in LDB3 have previously been implicated in dilated cardiomyopathy<sup>38,39</sup>. Here we found that exon 4 and exon 5/6 of LDB3 are mutually exclusively expressed and regulated by RBM20. Exon 4 of LDB3 has been implicated in binding of the glycolytic enzyme PGM1 and mutations in exon 4 have been shown to associate with DCM via impaired binding of PGM1<sup>40</sup>. The current work showed exon 4 to be down regulated in cardiac tissue from Rbm20 deficient rats and from the individual with the RBM20 missense mutation. This shift in LDB3 isoforms decreases the number of heart-specific PGM1 binding sites. It is conceivable that this may alter the recruitment of the glycolytic enzyme PGM1 to the Z-disk.

Our gene ontology analysis shows enrichment of genes involved in sarcomere organization and  $\alpha$ -actinin binding. This suggests a role for RBM20 in the concerted regulation of multiple proteins related to cardiac function in health and disease. Notably, while >15% of human genetic diseases have been attributed to mutations in *cis*-acting splice elements, only a few *trans* effects have been described to date<sup>5,41</sup>.

Dilated cardiomyopathy is a leading cause of heart failure and cardiac transplantation in Western countries and has been extensively studied<sup>42</sup>. While there is evidence of a substantial inherited contribution to DCM, there is also significant pleiotropy and reduced penetrance within families<sup>43</sup>. Numerous loci have been identified, and though the causal genes are known in only a small subset of these families, they include transcripts encoding sarcomeric contractile proteins, cytoskeletal proteins, nuclear membrane proteins, and the dystrophin associated glycoprotein complex<sup>44</sup>. The discovery of RBM20 as a novel *trans*-regulator of several of these and many other genes defines a hitherto unappreciated cause of cardiomyopathies.

In conclusion, our data suggest a model in which reduced activity of RBM20 results in altered isoforms expression of proteins that maintain sarcomeric structure and cardiac function – among them titin, CAMKII $\delta$ , LDB3, and CACNA1C. These changes may result in altered biomechanics, electrical activity, and signal transduction that ultimately lead to cardiomyopathy, fibrosis, arrhythmia, and sudden death. Our data highlight the importance of posttranscriptional regulation in physiological cardiac function and heart failure.

## METHODS

### Animal procedures

The rat strain with altered splicing was previously described<sup>16</sup>. We sacrificed splice deficient and control animals to harvest tissues for RNA-expression analysis (E18, P1, P20, P49, >P100) and the documentation of altered titin isoform expression (F2: P1-5, adults: 6m, 12m). For genotyping PCR and Southern blot we used DNA from liver samples. For expression analysis we extracted RNA from left ventricles. We evaluated cardiac dimensions and function by echocardiography of sedated rats (IP administration of 25-50 mg kg<sup>-1</sup> ketamine) using a Sonos 5500 ultrasonograph with a 15-MHz transducer (Philips, Andover MA). For functional calculations we followed American Society of Echocardiography guidelines. In the LV parasternal long axis 4-chamber view we derived fractional shortening (% FS) and ventricular dimensions. Detailed description of the cardiac phenotyping - including ECG readings, genotyping, and expression analysis is available in the online supplement. All experiments involving animals were carried out following institutional and NIH guidelines as approved by the Animal Care and Use Committee, University of Wisconsin-Madison or LaGeSo Berlin. Unless indicated otherwise, expression analysis was performed on 2 months old animals.

### Experimental crosses, genotyping, and genetic mapping

We kept affected animals with the titin splice defect on a mixed SD/F344 (SD/F) background. For mapping we crossed these animals with either F344 or BN rats to establish two independent F1 populations. We backcrossed each F1 cross to establish 2 independent N1 crosses. SNP genotyping was performed on genomic DNA using a 10K SNP assay as previously reported<sup>45</sup> using 23 DNA samples including three F1 (SD/F  $\times$  BN), four BN, and 16 affected splice deficient rats from the SD/F  $\times$  BN backcross<sup>46,47</sup>. The final dataset included a total of 4,391 informative SNPs that covered the autosomal genome with an average distance of 568 kb. We then tested for a shared SD/F allele between all 16 affected animals genotyped from the N1 (SD/F  $\times$  BN) backcross across all informative SNPs. We

calculated the probability of a given allele distribution using the one-sided binomial test under the null hypothesis of a random selection of the backcross individuals. For genome wide multiple testing we used the Benjamini Hochberg correction<sup>48</sup>. We confirmed mapping results by re-sequencing SNPs within the candidate interval (primer sequences available upon request).

### Histopathology

To detect fibrosis, we fixed hearts from 2 to 20 months old rats in 4% paraformaldehyde, paraffin-embedded, and stained with Masson's trichrome or Sirius red. The quantification of relative areas of connective tissue and cardiomyocytes is outlined in the supplement.

### Human studies

All human studies were approved by the institutional review boards and individuals gave informed consent. We evaluated a cohort of 120 unrelated subjects with idiopathic dilated cardiomyopathy (DCM) for mutations in RBM20 using PCR and Sanger sequencing. In the individual with the novel heterozygous RBM20 missense mutation (Ser635Ala), myocardial biopsies were obtained after diagnostic coronary angiography and immediately (< 10 s) frozen in liquid nitrogen. Furthermore we obtained cardiac tissue from subjects with DCM that do not carry mutations in RBM20. Both subjects were transplanted between 2003 and 2007 at the German Heart Center Berlin (DHZB). At this occasion cardiac samples were obtained and immediately frozen in liquid nitrogen.

### Tissue culture

We used HL-1 cells (mouse atrial myocytes), C2C12 (mouse myoblasts), and HEK 293 cells (human fibroblasts) for expression-, localization-, and RNA/protein-binding studies. For transfection of HEK293 we used Lipofectamine 2000. Only for the dual luciferase splice reporter assay C2C12 and HEK293 cells were transfected with TurboFect (Fermentas). We used adenoviral gene transfer to express Rbm20 vs. GFP in homozygous mutant neonatal cardiomyocytes. Additional information is available in the supplement.

### Global Splicing Analysis

We used cardiac rRNA-depleted poly(A)<sup>+</sup> mRNA from human cardiac biopsies and cardiac tissue from rats ( $n=3$  in each group of RBM20 homozygous deficient, heterozygous, and wildtype) to generate libraries, that were sequenced on a HiSeq 2000 instrument (Illumina) with 2x 100 bp PE –chemistry as detailed in the supplement. We used TopHat v1.3.1<sup>49</sup> to map reads to the reference genomes and cuffdiff (part of the Cufflinks 1.03 package<sup>50</sup>) to detect differential isoform processing for all genes as annotated by Ensembl. This approach allows direct testing of splicing with the cufflinks package without the need to predict isoforms de novo. We tested for differential splicing in pairwise comparisons for all three groups of animals (Rbm20 deficient, heterozygote, and homozygote wildtype) as well as for the individual with the RBM20 S635A missense mutation against two subjects with DCM that do not carry mutations in RBM20 each. Genes which were significantly differentially spliced in all comparisons were considered potential splicing targets of RBM20.

### Splice reporter assay

We inserted the firefly and renilla luciferase coding regions into an alternatively spliced and a constitutively expressed titin PEVK exon as indicated in Fig.2c. 48h after co-transfection with RBM20 expression vs. control plasmids, we used the Dual-Luciferase® Reporter Assay System (Promega) to determine the ratio of firefly to renilla luciferase activity as an indicator of exon-exclusion. Additional information and the validation by RT-PCR are available in the supplement.



## Protein analysis

We used SDS/agarose gel-electrophoresis of left ventricles or cultured cells homogenized in sample buffer (8 M urea, 2 M thiourea, 0.05 M Tris pH 6.8, 75 mM DTT, 3% SDS, 0.05% bromophenol blue) to separate titin isoforms. Additional information on pro- and eukaryotic expression of RBM20 and its subdomains, and generation of antibodies is available online.

## Accession Numbers

All rat and human RNA sequencing data have been submitted to the Sequencing Read Archive of the European Nucleotide Archive (SRA-ENA; accession numbers pending). The GenBank accession numbers for human and rat RBM20 are EU822950 and EU562301, respectively.

Additional methods and any associated references are available in the online version of the paper at <http://www.nature.com/naturemedicine/>.

## Supplementary Material

Refer to Web version on PubMed Central for supplementary material.

## Acknowledgments

We are grateful to B. Goldbrich, O. Hummel, S. Lubitz, S. Makino, G. Patone, S. Blachut, R. Plehm, S. Probst, S. Schmidt, and M. Wehle for expert technical assistance. R. Hetzer (Deutsches Herzzentrum Berlin) generously provided human cardiac tissue. Mammalian expression vectors for PTBP1 and HuD were gifts from R. Darnell, The Rockefeller University. Supported by the US National Institutes of Health HL77196 (M.L.G.) and HL075431 (C.A.M.), the Deutsche Forschungsgemeinschaft, Bonn, Germany and European Research Council StG282078 (M.G.), the German Ministry of Science and Education (NGFN-Plus Heart Failure Network) and EURATRANS (HEALTH-F4-2010-241504) (N.H.), and the American Heart Association (P.T.E).

## References

1. Chen M, Manley JL. Mechanisms of alternative splicing regulation: insights from molecular and genomics approaches. *Nat. Rev. Mol. Cell Biol.* 2009; 10:741–754. [PubMed: 19773805]
2. Lin S, Fu X-D. SR proteins and related factors in alternative splicing. *Adv. Exp. Med. Biol.* 2007; 623:107–122. [PubMed: 18380343]
3. Cooper TA, Wan L, Dreyfuss G. RNA and disease. *Cell.* 2009; 136:777–93. [PubMed: 19239895]
4. Lukong KE, Chang K.-wei, Khandjian EW, Richard S. RNA-binding proteins in human genetic disease. *Trends Genet.* 2008; 24:416–425. [PubMed: 18597886]
5. Wang GS, Cooper TA. Splicing in disease: disruption of the splicing code and the decoding machinery. *Nat Rev Genet.* 2007; 8:749–761. [PubMed: 17726481]
6. Gerull B, et al. Mutations of TTN, encoding the giant muscle filament titin, cause familial dilated cardiomyopathy. *Nat Genet.* 2002; 30:201–204. [PubMed: 11788824]
7. Makarenko I, et al. Passive stiffness changes caused by upregulation of compliant titin isoforms in human dilated cardiomyopathy hearts. *Circ Res.* 2004; 95:708–716. [PubMed: 15345656]
8. Lahmers S, Wu Y, Call DR, Labeit S, Granzier H. Developmental control of titin isoform expression and passive stiffness in fetal and neonatal myocardium. *Circ. Res.* 2004; 94:505–513. [PubMed: 14707027]
9. Opitz CA, Leake MC, Makarenko I, Benes V, Linke WA. Developmentally regulated switching of titin size alters myofibrillar stiffness in the perinatal heart. *Circ Res.* 2004; 94:967–975. [PubMed: 14988228]
10. Warren CM, Krzesinski PR, Campbell KS, Moss RL, Greaser ML. Titin isoform changes in rat myocardium during development. *Mech Dev.* 2004; 121:1301–1312. [PubMed: 15454261]

11. Yamasaki R, et al. Protein kinase A phosphorylates titin's cardiac-specific N2B domain and reduces passive tension in rat cardiac myocytes. *Circ Res.* 2002; 90:1181–1188. [PubMed: 12065321]
12. Cazorla O, et al. Differential expression of cardiac titin isoforms and modulation of cellular stiffness. *Circ Res.* 2000; 86:59–67. [PubMed: 10625306]
13. Wu Y, Peng J, Campbell KB, Labeit S, Granzier H. Hypothyroidism leads to increased collagen-based stiffness and re-expression of large cardiac titin isoforms with high compliance. *J. Mol. Cell. Cardiol.* 2007; 42:186–195. [PubMed: 17069849]
14. Krüger M, et al. Thyroid hormone regulates developmental titin isoform transitions via the phosphatidylinositol-3-kinase/AKT pathway. *Circ Res.* 2008; 102:439–47. [PubMed: 18096819]
15. Krüger M, Babicz K, von Frieling-Salewsky M, Linke WA. Insulin signaling regulates cardiac titin properties in heart development and diabetic cardiomyopathy. *J. Mol. Cell. Cardiol.* 2010; 48:910–916. [PubMed: 20184888]
16. Greaser ML, et al. Mutation that dramatically alters rat titin isoform expression and cardiomyocyte passive tension. *J Mol Cell Cardiol.* 2008; 44:983–991. [PubMed: 18387630]
17. Brauch KM, et al. Mutations in ribonucleic acid binding protein gene cause familial dilated cardiomyopathy. *J. Am. Coll. Cardiol.* 2009; 54:930–941. [PubMed: 19712804]
18. Li D, et al. Identification of novel mutations in RBM20 in patients with dilated cardiomyopathy. *Clin Transl Sci.* 2010; 3:90–97. [PubMed: 20590677]
19. Greaser ML, et al. Developmental changes in rat cardiac titin/connectin: transitions in normal animals and in mutants with a delayed pattern of isoform transition. *J Muscle Res Cell Motil.* 2005; 26:325–332. [PubMed: 16491431]
20. Gama-Carvalho M, et al. Targeting of U2AF65 to sites of active splicing in the nucleus. *J. Cell Biol.* 1997; 137:975–987. [PubMed: 9166400]
21. Okano HJ, Darnell RB. A hierarchy of Hu RNA binding proteins in developing and adult neurons. *J. Neurosci.* 1997; 17:3024–3037. [PubMed: 9096138]
22. Polydorides AD, Okano HJ, Yang YY, Stefani G, Darnell RB. A brain-enriched polypyrimidine tract-binding protein antagonizes the ability of Nova to regulate neuron-specific alternative splicing. *Proc. Natl. Acad. Sci. U.S.A.* 2000; 97:6350–6355. [PubMed: 10829067]
23. Wang D, Papp AC, Binkley PF, Johnson JA, Sadée W. Highly variable mRNA expression and splicing of L-type voltage-dependent calcium channel alpha subunit 1C in human heart tissues. *Pharmacogenet. Genomics.* 2006; 16:735–745. [PubMed: 17001293]
24. Zahler AM, Lane WS, Stolk JA, Roth MB. SR proteins: a conserved family of pre-mRNA splicing factors. *Genes Dev.* 1992; 6:837–847. [PubMed: 1577277]
25. Tacke R, Manley JL. Determinants of SR protein specificity. *Curr. Opin. Cell Biol.* 1999; 11:358–362. [PubMed: 10395560]
26. Lin S, Xiao R, Sun P, Xu X, Fu X-D. Dephosphorylation-dependent sorting of SR splicing factors during mRNP maturation. *Mol. Cell.* 2005; 20:413–425. [PubMed: 16285923]
27. Zhong X-Y, Ding J-H, Adams JA, Ghosh G, Fu X-D. Regulation of SR protein phosphorylation and alternative splicing by modulating kinetic interactions of SRPK1 with molecular chaperones. *Genes Dev.* 2009; 23:482–495. [PubMed: 19240134]
28. Toko H, et al. Ca<sup>2+</sup>-almodulin-dependent kinase IIdelta causes heart failure by accumulation of p53 in dilated cardiomyopathy. *Circulation.* 2010; 122:891–899. [PubMed: 20713897]
29. Cheng H, et al. Selective deletion of long but not short Cypher isoforms leads to late-onset dilated cardiomyopathy. *Hum. Mol. Genet.* 2011; 20:1751–1762. [PubMed: 21303826]
30. Tang ZZ, et al. Regulation of the mutually exclusive exons 8a and 8 in the CaV1.2 calcium channel transcript by polypyrimidine tract-binding protein. *J. Biol. Chem.* 2011; 286:10007–10016. [PubMed: 21282112]
31. Itoh-Satoh M, et al. Titin mutations as the molecular basis for dilated cardiomyopathy. *Biochem Biophys Res Commun.* 2002; 291:385–393. [PubMed: 11846417]
32. Neagoe C, et al. Titin isoform switch in ischemic human heart disease. *Circulation.* 2002; 106:1333–1341. [PubMed: 12221049]

33. Williams L, et al. Titin isoform expression in aortic stenosis. *Clin. Sci.* 2009; 117:237–242. [PubMed: 19154184]
34. Chaturvedi RR, et al. Passive stiffness of myocardium from congenital heart disease and implications for diastole. *Circulation.* 2010; 121:979–988. [PubMed: 20159832]
35. Ding J-H, et al. Dilated cardiomyopathy caused by tissue-specific ablation of SC35 in the heart. *EMBO J.* 2004; 23:885–96. [PubMed: 14963485]
36. Feng Y, et al. SRp38 regulates alternative splicing and is required for Ca(2+) handling in the embryonic heart. *Dev. Cell.* 2009; 16:528–538. [PubMed: 19386262]
37. Xu X, et al. ASF/SF2-regulated CaMKII $\delta$  alternative splicing temporally reprograms excitation-contraction coupling in cardiac muscle. *Cell.* 2005; 120:59–72. [PubMed: 15652482]
38. Vatta M, et al. Mutations in Cypher/ZASP in patients with dilated cardiomyopathy and left ventricular non-compaction. *J Am Coll Cardiol.* 2003; 42:2014–2027. [PubMed: 14662268]
39. Arimura T, et al. A Cypher/ZASP mutation associated with dilated cardiomyopathy alters the binding affinity to protein kinase C. *J. Biol. Chem.* 2004; 279:6746–6752. [PubMed: 14660611]
40. Arimura T, et al. Impaired binding of ZASP/Cypher with phosphoglucomutase 1 is associated with dilated cardiomyopathy. *Cardiovasc. Res.* 2009; 83:80–88. [PubMed: 19377068]
41. Matlin AJ, Clark F, Smith CWJ. Understanding alternative splicing: towards a cellular code. *Nat. Rev. Mol. Cell Biol.* 2005; 6:386–398. [PubMed: 15956978]
42. Roger VL, et al. Trends in heart failure incidence and survival in a community-based population. *JAMA.* 2004; 292:344–350. [PubMed: 15265849]
43. Mahon NG, et al. Echocardiographic evaluation in asymptomatic relatives of patients with dilated cardiomyopathy reveals preclinical disease. *Ann Intern Med.* 2005; 143:108–115. [PubMed: 16027452]
44. Liew CC, Dzau VJ. Molecular genetics and genomics of heart failure. *Nat Rev Genet.* 2004; 5:811–825. [PubMed: 15520791]
45. Saar K, et al. SNP and haplotype mapping for genetic analysis in the rat. *Nat Genet.* 2008; 40:560–566. [PubMed: 18443594]
46. Hardenbol P, et al. Multiplexed genotyping with sequence-tagged molecular inversion probes. *Nat Biotechnol.* 2003; 21:673–678. [PubMed: 12730666]
47. Hardenbol P, et al. Highly multiplexed molecular inversion probe genotyping: over 10,000 targeted SNPs genotyped in a single tube assay. *Genome Res.* 2005; 15:269–275. [PubMed: 15687290]
48. Benjamini Y, Hochberg Y. Controlling the false discovery rate: a practical and powerful approach to multiple testing. *J Roy Statist Soc Ser B.* 1995; 57:289–300.
49. Trapnell C, Pachter L, Salzberg SL. TopHat: discovering splice junctions with RNA-Seq. *Bioinformatics.* 2009; 25:1105–1111. [PubMed: 19289445]
50. Trapnell C, et al. Transcript assembly and quantification by RNA-Seq reveals unannotated transcripts and isoform switching during cell differentiation. *Nat. Biotechnol.* 2010; 28:511–515. [PubMed: 20436464]

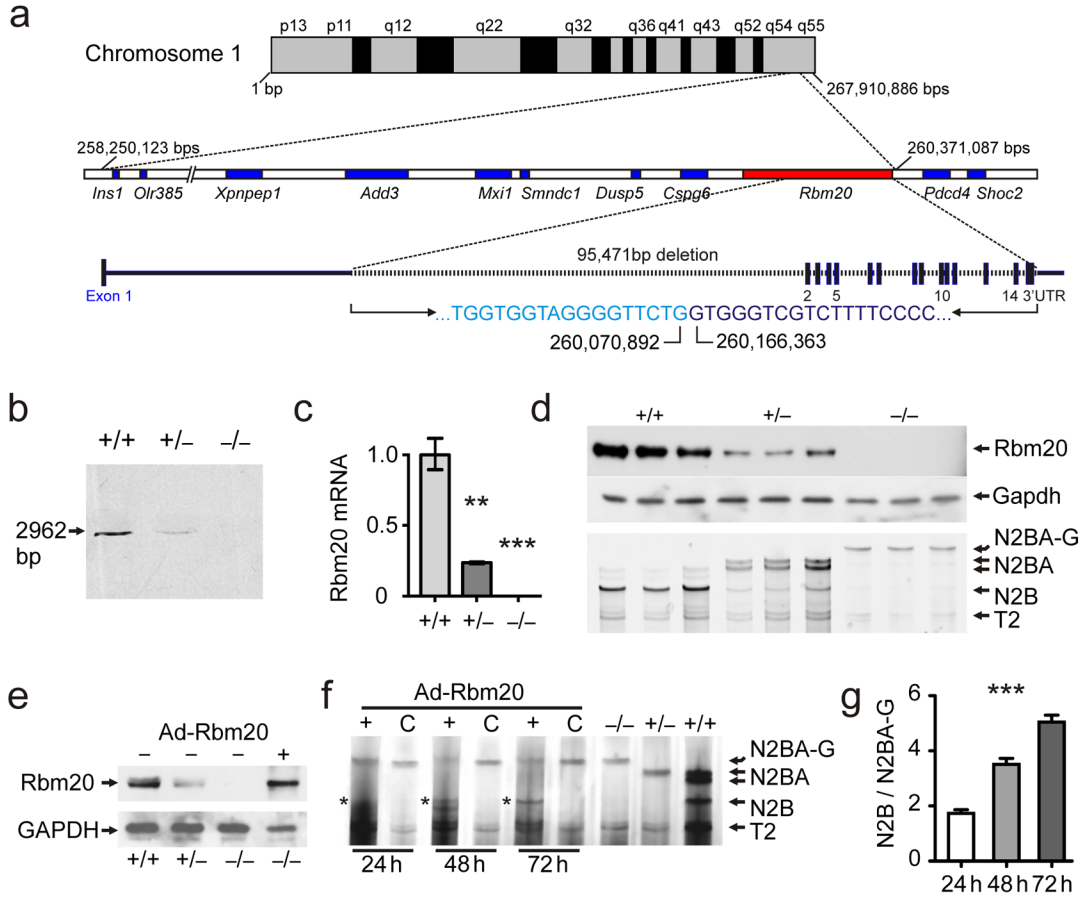


**Figure 1.**

Mapping of the titin splice defect and validation of RBM20 as the affected gene. **(a)** In a splice deficient rat strain the QTL resides in a 2.1 Mbps interval on the long arm of chromosome 1 (1q55). The coding sequence of all known genes included in the interval was unchanged except for the *Rbm20* gene with a 95 kb deletion that eliminates all exons following exon 1. **(b)** Southern-blot of genomic DNA confirms the deletion with the loss of a 3 kb internal *HindIII* fragment in homozygous (-/-) and a reduced signal in heterozygous (+/-) compared to wildtype (+/+) rats. **(c)** *Rbm20* RNA levels normalized to 18S and wildtype levels reflect the changes documented by Southern blot with a 76% reduction in the heterozygote and no expression in the homozygote (< 1%). *N* = 9. *P* < 0.01 (\*\*\*) and *P* < 0.001 (\*\*). **(d)** With reduced levels of *Rbm20*, there is a shift from the shorter N2B-titin to the larger N2BA isoforms (heterozygotes) and N2BA-G (homozygote mutant) as determined by agarose gel electrophoresis. T2 refers to a proteolytic fragment that is independent of the titin isoform. *Gapdh* was used as a loading control for the western blot. **(e)** Adenoviral gene transfer into homozygous deficient cardiomyocytes leads to reexpression of RBM20 in homozygous deficient neonatal cardiomyocytes (last lane). **(f)** Treatment of neonatal RBM20 deficient cardiomyocytes with *Rbm20*-vs. control-virus (C) resulted in a reproducible downregulation of the larger N2BA isoform starting from 24h after infection and upregulation of the N2B isoform (asterisks). **(g)** Quantification of titin isoform expression shows a linear increase in the N2B/N2BA-G ratio from 24 to 72h after infection with the *Rbm20* adenovirus. One-Way-Anova test *P* < 0.001 (\*\*\*)

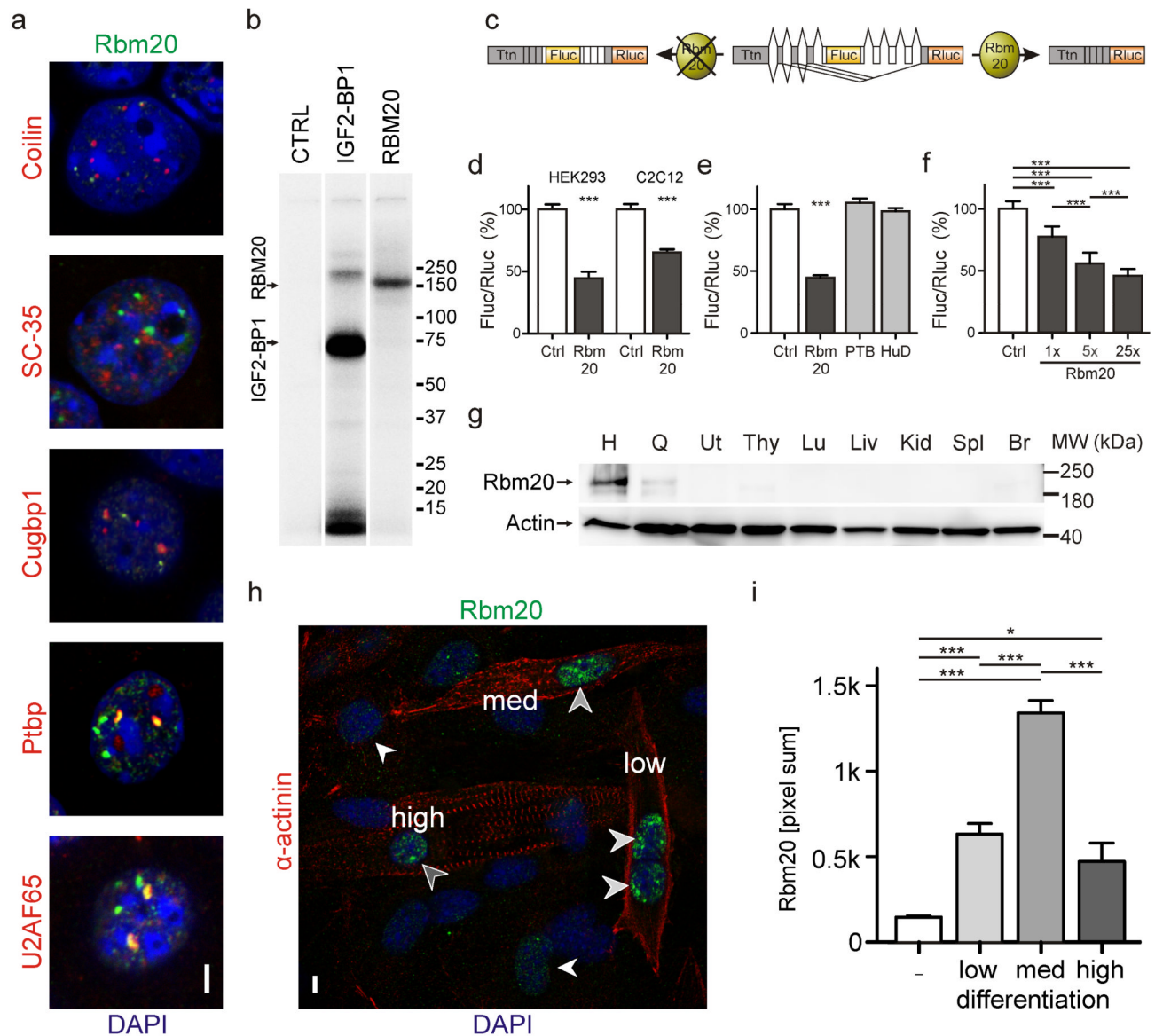


**Figure 2.**

Analysis of RBM20 expression and function. **(a)** In nuclei of HL1 cells Rbm20 partially colocalizes with the splice factor U2AF65 and Ptpbp1, but not with additional splice factors tested (Cugbp1 and SC-35) or coilin, a marker for Cajal bodies. (Scale bar 5  $\mu$ m). **(b)** Autoradiogram of 5'-32P-labeled RNA-protein immunoprecipitates (IPs) derived from RBM20 and IGF2BP1 overexpressing HEK293 cells. After cultivation in media containing a photoreactive nucleoside and UV-crosslinking both the positive control IGF2BP1 and RBM20 bound RNA. Untransfected HEK293 cells were used as a negative control (CTRL). **(c)** Specific activity of RBM20 on titin RNA was monitored in a cell-based splice reporter assay utilizing the 5'-PEVK exons, firefly and renilla luciferase (Fluc and Rluc). Expression of RBM20 leads to exclusion of the Fluc containing exon. Black lines indicate exon junctions as determined by sequencing RT-PCR products derived from cells that express the reporter construct with and without RBM20. **(d)** The ratio of Fluc to Rluc reflects splice activity and decreased with expression of RBM20 in both HEK293 cells and in C2C12 myoblasts. **(e)** The control RNA binding proteins and splice factors PTBP1 and HuD did not

interfere with alternative splicing. **(f)** Transfection of increasing amounts of RBM20 (1x, 5x, or 25x excess of the expression construct) led to improved excision of the Fluc reporter. **(g)** Rbm20 protein expression at 2 months of age is largely restricted to cardiac and skeletal muscle (H, Heart, Q, Quadriceps, Ut Uterus, Thy Thymus, Lu Lung, Liv Liver, Kid Kidney, Spl Spleen, Br Brain). Actin shows proper regulation in muscle vs. non-muscle tissues and was used as a loading control. **(h)** C2C12 cells were stained for  $\alpha$ -actinin (red) as a marker of sarcomere maturation and staged for low, medium, and high differentiation based on the fluorescence pattern. Rbm20 expression (green) was restricted to the nuclei (DAPI, blue). (Scale bar 5  $\mu$ m). **(i)** Quantification of Rbm20 expression at four levels of cellular differentiation as shown in (h). The ratio of total intensity distribution over the nuclear area was lowest in undifferentiated cells (-), intermediate with both low and high differentiation (low, high), and highest at intermediate differentiation (med). Significance levels at  $P = 0.05$  (\*) and  $P < 0.001$  (\*\*\*) are indicated ( $N > 15$  per group).

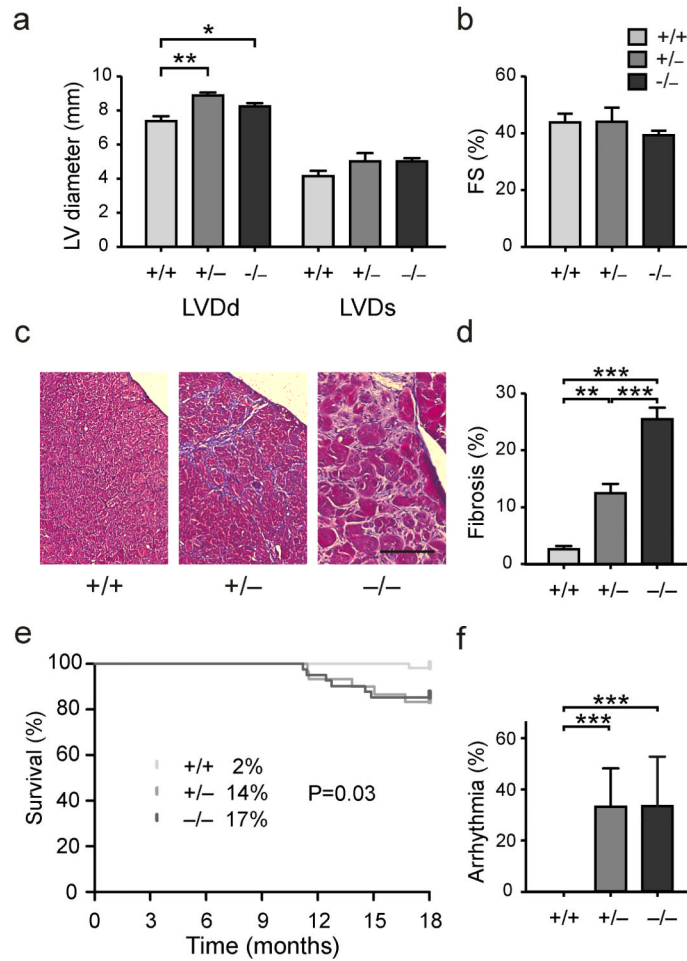


**Figure 3.**

Signs of cardiomyopathy with arrhythmia and sudden death in *Rbm20* deficient rats. **(a, b)** Left ventricular diameter in diastole (LVDd) as determined by echocardiography was increased in both heterozygous and homozygous mutants as a sign of dilated cardiomyopathy ( $P < 0.05$ ;  $n = 15$ ). Changes in LV diameter in systole (LVDs) and fractional shortening (FS), a parameter of contractile function, did not reach statistical significance. **(c)** Subendocardial fibrosis was present in heterozygote mutants (+/-) as indicated by the trichrome staining (blue). The fibrotic area was increased and compacted in the homozygous hearts (-/-). Size bar = 100  $\mu\text{m}$ . **(d)** Interstitial fibrosis was significantly increased in LV from heterozygous (13% fibrotic area) and homozygous (26%) as compared to wildtype hearts (3%).  $N = 13$ . **(e, f)** Increased inducibility of arrhythmia in both hetero- and homozygotes was associated with an increase in sudden death starting from 10 months of age. Deaths in percent are indicated at 18 months of age. Log-rank (Mantel-Cox) test  $P = 0.03$ ;  $n = 130$ .

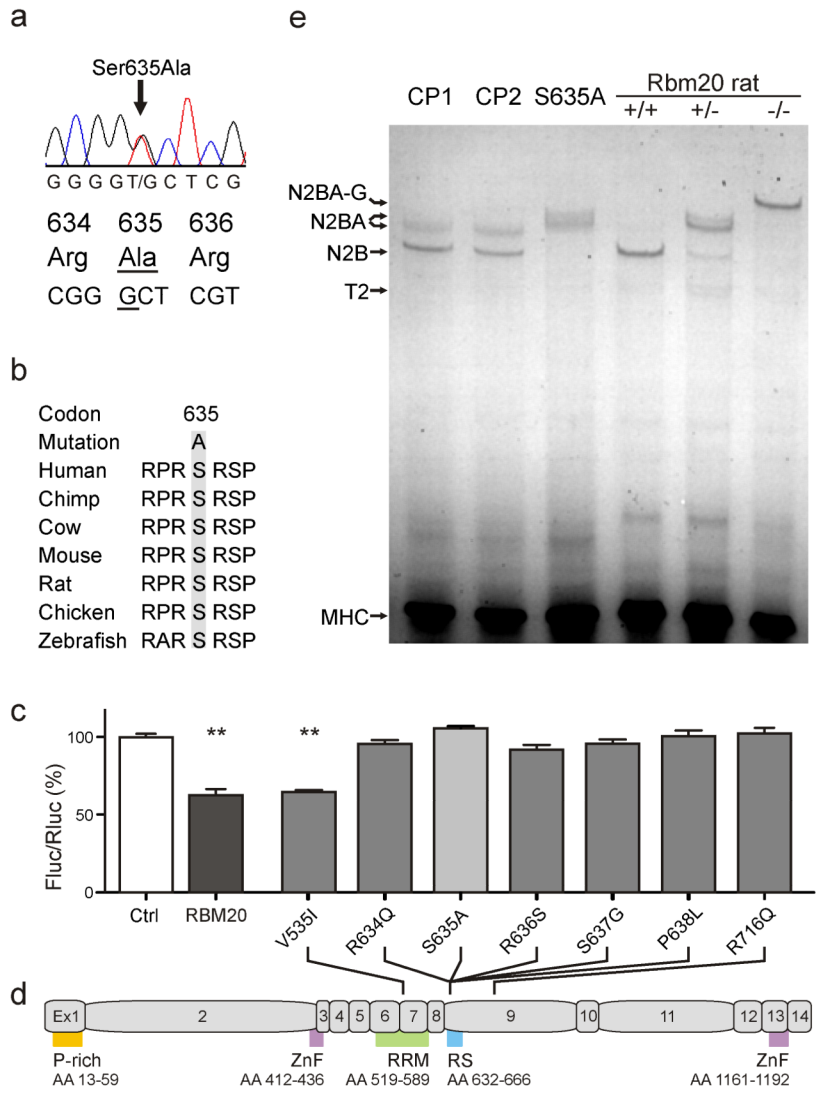


**Figure 4.** (a) Identification of a novel RBM20 mutation in a human with severe cardiomyopathy and arrhythmia that leads to a change of serine to alanine within the RS domain. (b) The region affected is highly conserved between species. (c, d) The newly identified S635A mutation renders RBM20 inactive in our splice reporter assay – along with all previously described RBM20 mutations in exon 9. V535I resides in exon 6 and does not affect reporter activity. *N*=8; SEM. P-rich, proline rich; ZnF, Zinc Finger; RRM RNA-recognition-motif; RS, Arginine-Serine rich. (e) RBM20 deficiency leads to changes in titin isoform expression as determined by SDS-agarose gel electrophoresis. Compared to control subjects with cardiomyopathy of unrelated cause (CP1 and CP2), the RBM20 deficient individual (S635A) expresses a larger cardiac titin isoform. A similar increase is seen in the heterozygous mutant rat, while homozygote rats express the larger N2BA isoforms.



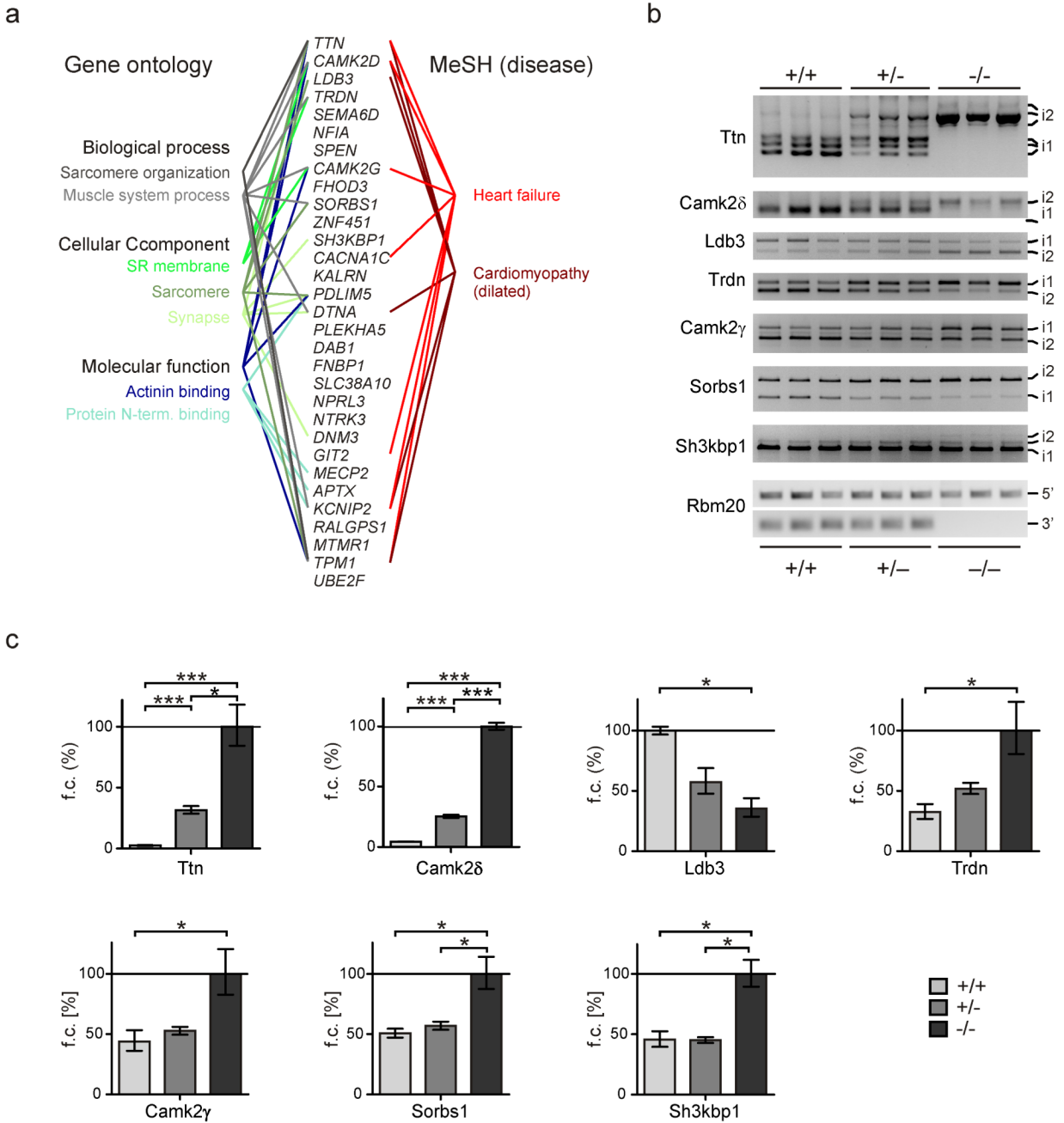


**Figure 5.** Characterization of RBM20 dependent isoform expression. **(a)** A conserved set of 31 genes with RBM20 dependent alternative splicing was identified by next-generation sequencing of humans and rats, which includes titin as the most differentially spliced gene. An enrichment analysis of these candidate substrates using gene ontology and medical subject heading terms (MeSH) suggests a role of RBM20 in regulating protein isoforms within the sarcomere and sarcoplasmic reticulum of striated muscle and a relation to heart failure and cardiomyopathy. **(b)** Alternative splicing of genes with high  $\Delta$ PSI values as determined by RNA-seq was confirmed by RT-PCR. The shift between isoforms predominant in the wildtype (i1) and those primarily expressed in the mutant (i2) was strongest in homozygote Rbm20 deficient rats (-/-). Heterozygotes showed an intermediate effect (+/-). Rbm20

exon 1 (5') and 6 to 7 (3') were amplified as controls with only 3' exons deleted in the mutant. PCR fragments were sequence verified as indicated in the Supplement Figure 9. (c) Relative exon expression was determined by qRT-PCR. Exons analyzed for Titin, CamkII $\delta$ , Trdn, Camk2 $\gamma$ , Sorbs1, Sh3kbp1 were included in transcripts of homozygotes (-/-) at higher levels. The alternatively spliced exon tested for Ldb3 was increasingly included in the wildtype (elevated expression in +/+). The strong effects of titin and CamkII $\delta$  were confirmed by larger differences in exon inclusion and significance between all groups. Significance levels at  $P \leq 0.05$  (\*) and  $P \leq 0.001$  (\*\*\*) are indicated ( $n = 3$  per group). Primers used are indicated in the supplementary figure S8.

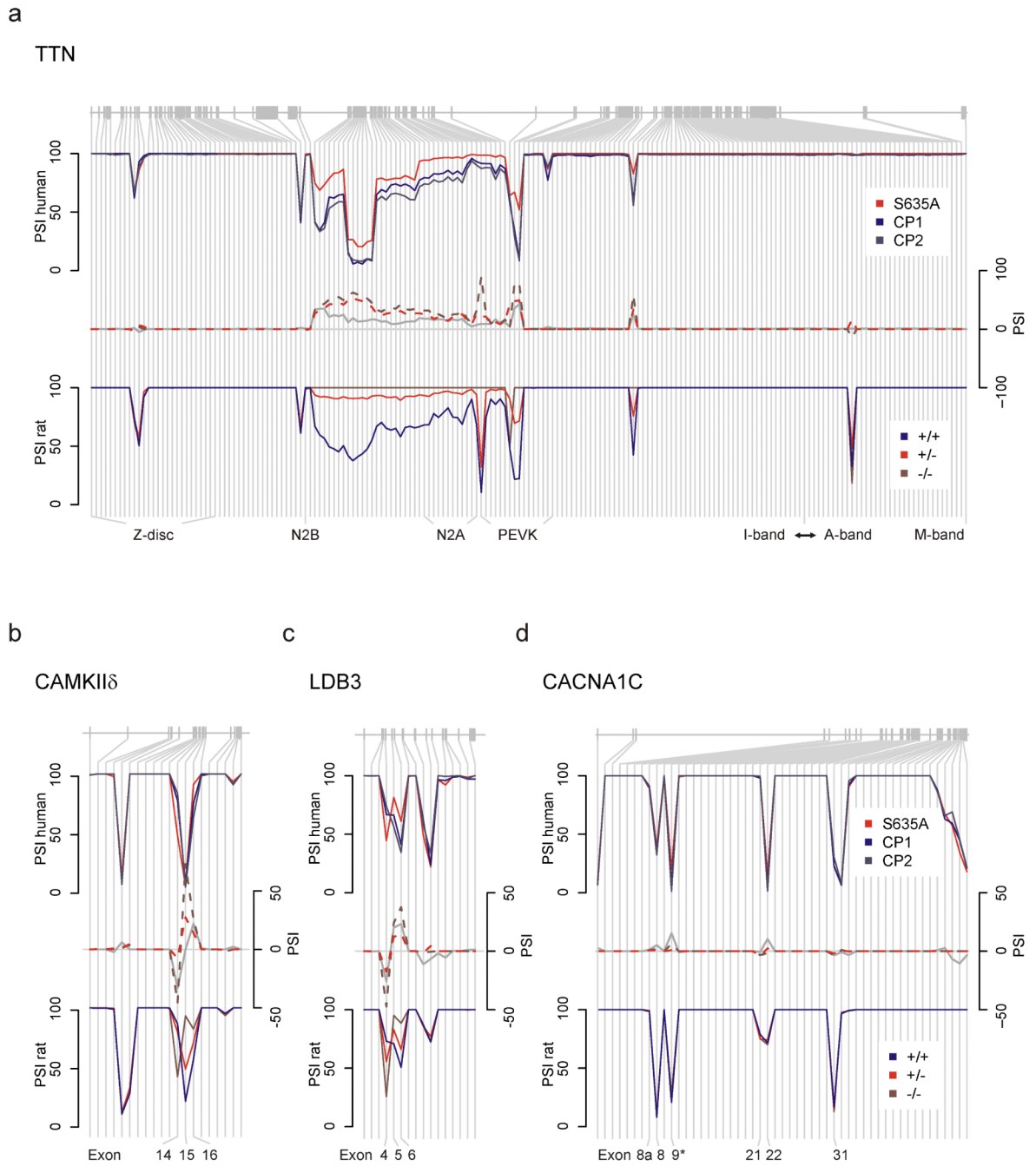


**Figure 6.** Alignment of orthologous rat and human exons for Titin, CAMKII $\delta$ , LDB3, and CACNA1C to compare RBM20 dependent isoform expression. PSI scores of humans are indicated in red for the RBM20 deficient individual (S635A) and in blue for two control subjects with DCM of unrelated cause (CP1 and CP2). The average PSI of 3 rats per genotype is provided below and aligned to the human exon structure (wildtype blue; heterozygote light red, homozygote dark red). The resulting  $\Delta$ PSI for human (continuous line) and rat (dashed lines; light red wildtype vs. heterozygotes, dark red wildtype vs. homozygotes) show highly conserved deflections up (additional inclusion of exons) and down (exon skipping) in differentially spliced regions across species with heterozygotes at intermediate levels. (a)

Titin is predominantly spliced in the elastic region extending from the N2B to the PEVK region. The 5' and 3' regions are unaffected as indicated by  $\Delta$ PSI curves approaching 0. Both alternatively spliced and constitutive regions are conserved between species. **(b)** CAMKII $\delta$  exons 14–16 are mutually exclusive and differentially regulated by RBM20 with exon14 up-regulated in the control and exons 15 and 16 in the mutant (indicated by the crossing of PSI lines between exon 14 and 15). **(c)** LDB3 undergoes a similar exon switch that affects exon 4 (included in the control) and exons 5 and 6 excluded with reduced RBM20 activity. **(d)** CACNA1C is consistently regulated in human and rat for the majority of alternatively spliced exons (8, 9\*, 22, 31) but differences in inclusion rates are small with  $\Delta$ PSI of <10.